



ELSEVIER

Neurobiology of Aging xxx (2008) xxx–xxx

**NEUROBIOLOGY
OF
AGING**

www.elsevier.com/locate/neuaging

Up-regulation of divalent metal transporter 1 is involved in 1-methyl-4-phenylpyridinium (MPP⁺)-induced apoptosis in MES23.5 cells

Shuzhen Zhang¹, Jun Wang¹, Ning Song, Junxia Xie*, Hong Jiang**

Department of Physiology, Medical College of Qingdao University, No. 308 Ningxia Road, Qingdao 266071, China

Received 6 July 2007; received in revised form 29 October 2007; accepted 23 November 2007

Abstract

Apoptosis has been identified as one of the important mechanisms involved in the degeneration of dopaminergic neurons in Parkinson's disease (PD). Our previous study showed increased iron levels in the substantia nigra as well as loss of dopaminergic neurons in 1-methyl-4-phenyl-1,2,3,6-tetrahydropyridine-induced PD mouse models. 1-Methyl-4-phenylpyridinium (MPP⁺) is commonly used to establish a cellular model of PD. Although intracellular iron plays a crucial role in MPP⁺-induced apoptosis, the molecular mechanism linking increased iron and MPP⁺-induced neurodegeneration is largely unknown. In the present study, we investigate the involvement of divalent metal transporter 1 (DMT1) that accounts for the ferrous iron transport in MPP⁺-treated MES23.5 cells. In the treated cells, a significant influx of ferrous iron was observed. This resulted in a decreased mitochondrial membrane potential. Additionally, an elevated level of ROS production and activation of caspase-3 were also detected, as well as the subsequent cell apoptosis. These effects could be fully abolished by iron chelator desferal (DFO). Increased DMT1 (–IRE) expression but not DMT1 (+IRE) accounted for the increased iron influx. However, there were no changes for iron regulatory protein 1 (IRP1), despite decreased expression of IRP2. Iron itself had no effect on IRP1 and IRP2 expression. Our data suggest that although DMT1 mRNA contains an iron responsive element, its expression is not totally controlled by this. MPP⁺ could up-regulate the expression of DMT1 (–IRE) in an IRE/IRP-independent manner. Our findings also show that MPP⁺-induced apoptosis in MES23.5 cells involves DMT1-dependent iron influx and mitochondria dysfunction.

© 2007 Elsevier Inc. All rights reserved.

Keywords: Divalent metal transporter 1 (DMT1); Apoptosis; Parkinson's disease; Iron; Iron regulatory protein (IRP); Iron chelator

1. Introduction

Elevated iron levels are found in the substantia nigra (SN), the brain region composed of the dopaminergic neurons that undergo selective neurodegeneration in Parkinson's disease (PD) (Dexter et al., 1989, 1993; Riederer et al., 1989; Rouault, 2001; Xie et al., 2003; Gotz et al., 2004;

Wang et al., 2004, 2007; Gal et al., 2005; Hardy et al., 2005; Berg and Hochstrasser, 2006; Jiang et al., 2006, 2007). Accessible intracellular ferrous iron can react with hydrogen peroxide to produce the hydroxyl radicals that in turn can damage proteins, nucleic acids and lipids, leading to cell death (Kamp et al., 2002; Andersen, 2004). Since apoptosis has been implicated as one of the important mechanisms leading to the death of dopaminergic neurons in PD, 1-methyl-4-phenylpyridinium (MPP⁺) is employed to produce a PD cell model in vitro in this study. Our aim is to elucidate whether iron is involved in MPP⁺-induced apoptosis. MPP⁺, a metabolite of 1-methyl-4-phenyl-1,2,3,6-tetrahydropyridine (MPTP), is selectively transported into dopaminergic neurons through the dopamine transporter and concentrated into mitochondria. MPP⁺-induced cell apoptosis involves multiple mechanisms, including complex I

Abbreviations: SN, substantia nigra; PD, Parkinson's disease; MPP⁺, 1-methyl-4-phenylpyridinium; MPTP, 1-methyl-4-phenyl-1,2,3,6-tetrahydropyridine; DMT1, divalent metal transporter 1; IRE, iron responsive element; TfR, transferrin receptor; UTR, untranslated region; DFO, desferal; IRP, iron regulatory protein.

* Corresponding author.

** Corresponding author. Tel.: +86 532 83780191; fax: +86 532 83780136.

E-mail address: jhkyk06@gmail.com (H. Jiang).

¹ These authors contribute equally to this work.

0197-4580/\$ – see front matter © 2007 Elsevier Inc. All rights reserved.

doi:10.1016/j.neurobiolaging.2007.11.025

Please cite this article in press as: Zhang, S., et al., Up-regulation of divalent metal transporter 1 is involved in 1-methyl-4-phenylpyridinium (MPP⁺)-induced apoptosis in MES23.5 cells, *Neurobiol Aging* (2008), doi:10.1016/j.neurobiolaging.2007.11.025

inhibition, inhibition of calcium homeostasis, opening of the mitochondrial transition pore, etc. (Kalivendi et al., 2003; Deguil et al., 2007). In our previous study, we found elevated iron levels in the SN of the MPTP-induced PD mouse models, as well as the loss of dopaminergic neurons. Up-regulation of divalent metal transporter 1 (DMT1) was also observed (Jiang et al., 2003). Although transferrin receptor (TfR)-induced iron uptake has been reported to play a role in MPP⁺ toxicity (Kalivendi et al., 2003), whether other iron transporters are involved is still unknown.

DMT1, also known as natural resistance associated macrophage protein 2 (Nramp2), is a widely expressed transmembrane protein (Gunshin et al., 1997). Four DMT1 isoforms are distinguished arising from their variant mRNA transcripts that vary both at their 5'-untranslational region (UTR) (starting from exon 1A or exon 1B) and their 3'-UTR (depending on the presence or absence of the iron responsive element (IRE) in the 3'-ends) (Lee et al., 1998; Hubert and Hentze, 2002; Mackenzie et al., 2007). High levels of DMT1 expression are found in some nuclei of the basal ganglia, particularly the caudate nucleus, putamen, and SN, indicating that DMT1 may account for the high iron levels in these regions (Gunshin et al., 1997; Burdo et al., 2001; Huang et al., 2004; Knutson et al., 2004; Ke et al., 2005). DMT1 is also highly expressed in the SN in PD (Andrews et al., 1999; Jiang et al., 2003; Moos and Morgan, 2004), indicating that disrupted expression of DMT1 might be involved in the iron accumulation in this area.

Due to the suggested involvement of DMT1 in PD, we investigate the expression of DMT1 (+IRE) and DMT1 (−IRE) in MPP⁺-treated MES23.5 cells, a dopaminergic cell line hybridized from murine neuroblastoma-glioma N18TG2 cells with rat mesencephalic neurons exhibits several properties similar to the primary neurons originated from the SN (Crawford et al., 1992). Results showed that up-regulation of DMT1 (−IRE) might account for the increased iron influx due to the MPP⁺ treatment. DMT1 (+IRE) was found to be unchanged. Increased intracellular ferrous iron causes the ultimate damage to the mitochondria, generation of ROS, and activation of caspase-3, which leads to cell apoptosis. Iron chelator desferal (DFO) could protect cells from MPP⁺-induced apoptosis.

2. Methods

2.1. Materials

Unless otherwise stated, all chemicals were purchased from Sigma Chemical Co. (St. Louis, MO, USA). The primary antibodies against DMT1 ± IRE were purchased from the ADI (ADI, San Antonio, TX, USA). Calcein-AM was from Molecular Probes (Molecular Probes Inc., Carlsbad, CA, USA). Dulbecco's modified Eagle's medium Nutrient Mixture-F12 (Ham) (DMEM/F12) was from Gibco (Gibco, Grand Island, NY, USA). The PE-conjugated mon-

oclonal active caspase-3 antibody apoptosis kit was from BD Bioscience Company (BD Biosciences pharmingen, Franklin Lakes, NJ, USA). Hoechst 33258 was from Beyotime (Jiangsu, China). All other chemicals and reagents were of the highest grade available from local commercial sources.

2.2. Cell culture

MES23.5 cells were offered by Dr. Wei-dong Le (Baylor College of Medicine, TX, USA). They were cultured in DMEM/F12 containing Sato's components growth medium supplemented with 5% fetal bovine serum (FBS), 100 units/mL penicillin and 100 µg/mL streptomycin at 37 °C, in a humid 5% CO₂, 95% air environment. For experiments, cells were seeded at a density of 1 × 10⁵/cm² in the plastic flasks or on glass coverslips.

2.3. MTT assay

MES23.5 cells were seeded in a 96-well plate at a density of 2 × 10⁴ cells/well. After attachment, MPP⁺ (final concentration 0–160 µmol/L) was added in DMEM/F12 without serum for the subsequent 24 h, then cells were incubated in MTT (5 mg/mL) for 4 h and cell injury was measured by colorimetric assay (TECAN, Austria).

2.4. Calcein loading of cells and ferrous iron influx assay

Ferrous iron influx into MES23.5 cells was determined by the quenching of calcein fluorescence as described before (Breuer et al., 1995; May et al., 1999; Wetli et al., 2006; Song et al., 2007). Cells were seeded to coverslips and grown in serum-free medium with MPP⁺ (5 µmol/L) for 24 h alone or followed by 1 mmol/L DFO treatment for 2 h (Tenopoulou et al., 2005). They were then incubated with calcein-AM (0.5 µmol/L final concentration) in HEPES-buffered saline (HBS, 10 mmol/L HEPES, 150 mmol/L NaCl, pH 7.4) for 30 min at 37 °C. The excess calcein on the cell surface was washed out 3 times with HBS. The cover slips were then mounted in a perfused chamber. Calcein fluorescence was recorded at 488 nm excitation and 525 nm emission wavelengths, and fluorescence intensity was measured every 3 min for 10 times while perfusing with 1 mmol/L ferrous iron (ferrous sulfate in ascorbic acid solution, 1:44 molar ratio, pH 6.0) (Picard et al., 2000), prepared immediately prior to the experiments. Ascorbic acid maintained the reduced status of ferrous iron, in addition, ascorbate acted as a chelator to maintain the iron in solution. The mean fluorescence signal of 35–40 single cells in four separate fields was monitored at 200× magnification and processed with Fluoview 5.0 Software.

2.5. Detection of mitochondrial transmembrane potential ($\Delta\psi_m$)

Changes in the mitochondrial membrane potential with various treatment in MES23.5 cells were measured by rhodamine123 using flow cytometry (Becton Dickinson, USA) as described before (Zhu and Liu, 2004; Sanelli et al., 2007). The uptake of rhodamine123 into mitochondria is an indicator of the $\Delta\psi_m$. Cells treated with vehicle, MPP⁺, and MPP⁺ followed by DFO were incubated in 100 $\mu\text{mol/L}$ ferrous iron (pH 6.0) for 3 h, and then incubated with rhodamine 123 in a final concentration of 5 $\mu\text{mol/L}$ for 30 min at 37 °C. After washing twice with HBS, fluorescence was recorded at 488 nm excitation and 525 nm emission wavelengths.

2.6. Reactive oxygen species (ROS) assay

Intracellular ROS were examined using 2',7'-dichlorodihydrofluorescein diacetate (H₂DCF-DA) as described before (Ryu et al., 2004; Yang et al., 2007). Cells treated as described above were incubated in HBS containing H₂DCF-DA (5 μM). Then ferrous iron (pH 6.0) was added for 3 h, followed by washing twice with PBS. The fluorescence signals were measured with 488 nm excitation and 525 nm emission wavelengths.

2.7. Active caspase-3 assay

Active caspase-3 assay was measured according to the manufacturer's protocol (BD Pharmingen™, BD Biosciences pharmingen, USA). Cell treatment was the same as the above. After washing twice with cold PBS, cells were resuspended in Citofix/Cytoperm™ solution at a concentration of 1×10^6 cells/0.5 mL. After incubation on ice for 20 min, cells were washed with Perm/washing buffer twice, then incubated in Perm/wash buffer with antibody (1:5). After washing once with Perm/washing buffer, cells were resuspended with 0.5 mL Perm/washing buffer and analyzed by flow cytometry. The extent of apoptosis was determined by counting the number of active caspase-3 immunoreactive cells as a percentage of total MES23.5 cells using Cellquest Software.

2.8. Hoechst 33258 stains

Nuclear morphology was detected using the method described before (Yao et al., 2006). MES23.5 cells were seeded on sterile cover glasses placed in the six-well plates at a density of 1.0×10^4 cells/cm². After various treatments, cells were fixed, washed twice with PBS and stained with Hoechst 33258 staining solution according to the manufacturer's instructions (Beyotime, Jiangsu, China). Cells were then examined and immediately photographed under a fluorescence microscope (Olympus, Japan), with an excitation wavelength of 330–380 nm. Apoptotic cells were defined on the basis of nuclear morphology changes, such as chromatin

condensation and fragmentation. The total number of condensed cells was counted manually by researchers blinded to the treatment schedule using unbiased stereology (West et al., 1991) and a fluorescence Olympus microscope (Olympus, Japan). For each well, we delineated a 400 μm^2 frame and counted all condensed and normal nuclei with at least 10 different fields in one well. Average sum of condensed and normal nuclei was calculated per well. The data were expressed as a percentage of condensed nuclear number to the total number.

2.9. Western blots analysis

Cells were incubated with MPP⁺ (5 $\mu\text{mol/L}$) for 24 h. After three washes with cold PBS, cells were digested directly on culture plates with RIPA lysis buffer (50 mmol/L Tris-HCl, 150 mmol/L NaCl, 1% Nonidet-40, 0.5% sodium deoxycholate, 1 mmol/L EDTA, 1 mmol/L PMSF) with protease inhibitors (pepstatin 1 $\mu\text{g/mL}$, aprotinin 1 $\mu\text{g/mL}$, leupeptin 1 $\mu\text{g/mL}$) for 30 min on ice and the insoluble material was removed by centrifugation (12000 rpm, 20 min, 4 °C). Sixty microgram total proteins were separated using 10% SDS-polyacrylamide gels and then transferred to PVDF membranes. Blots were probed with anti-DMT1 (\pm IRE) polyclonal antibody (ADI, 1:2000). Blots were also probed with anti- β -actin monoclonal antibody (Sigma, 1:10,000) as a loading control. Cross-reactivity was visualized using ECL Western blotting detection reagents and then analyzed through scanning densitometry by a Tanon Image System.

2.10. Total RNA extraction and quantitative and semiquantitative PCR

Total RNA was isolated by using Trizol Reagent (Invitrogen) from MES23.5 treated as described above according to the manufacturer's instructions. Then 2 μg total RNA was reversed transcribed in a 20 μL reaction using reverse-transcription system (Promega). Quantitative RCR was employed to detect the changes of DMT1 (\pm IRE). TaqMan probe and the primers were designed to sequences using the default settings of Primer Express 2.0 (PE Applied Biosystems). Each set of primers was used with a TaqMan probe labeled at the 5'-end with the 6-carboxyfluorescein (FAM) reporter dye and at the 3'-end with the 6-carboxy-tetramethylrhodamine (TAMRA) quencher dye. The following primers and probes were employed for DMT1 (+IRE) or DMT1 (–IRE), respectively: DMT1 (+IRE) forward 5'-TGGCTGTACGAGTGCTTACA-3', reverse 5'-CCATGGCCTTGGACAGCTATT-3', probe 5'-TTACCCTGTAGCATTAGGCAGCACC-3'; DMT1 (–IRE) forward 5'-AAGCCCTTTTGTGCCAAGTGT-3', reverse 5'-ACCCATTCACAGCCGTTAGCT-3', probe 5'-CAAATGTTTTGAACCAAGGCGAAGA-3'. Rat GAPDH gene was used as the reference: forward 5'-CCCCAATGTATCCGTTGTG-3', reverse 5'-GTAGCCCAGGATGCCCTTTAGT-3', probe 5'-

TCTGACATGCCGCCTGGAGAAACC-3'. Reactions were carried out on an ABI PRISM[®] 7500 Sequence Detection System using the relative quantification option of the SDS1.2.1 software (Applied Biosystems). Each reaction was run in triplicate with 2 μ L sample in a total volume of 20 μ L with primers and probes to a final concentration of 0.25 μ mol/L. A passive reference dye, ROXII, was used to normalize the reporter signal. Amplification and detection were performed with the following conditions: an initial hold at 95 °C for 10 s followed by 40 cycles at 95 °C for 5 s and 60 °C for 45 s.

To compare the changes of IRP1 and IRP2, we used the following primers for PCR: rat IRP1 forward primer, 5'-TTACCAAGCACCTCCGACAA-3'; backward primer, 5'-AATCCTGCGCCTAACATCA-3'. The amplified IRP1 fragment was 562 bp. Rat IRP2 forward primer, 5'-GCCGAAACTCAGGAACA-3'; backward primer, 5'-GTCACATTGTCAACAGGGA-3'. The amplified IRP2 fragment was 622 bp. Mouse GAPDH was used as a loading control: forward primer, 5'-TTCACCACCATGGAGAAGGC-3'; backward primer, 5'-GGCATGGACTGTG GTCATGA-3'. The amplified mouse GAPDH fragment was 236 bp. Thermocycling was carried out as follows: 94 °C for 5 min, then 35 cycles of 94 °C for 30s, 45 °C or 62 °C for 30s, 72 °C for 1 min, followed by 72 °C for 10 min.

2.11. Statistical analysis

Results are presented as mean \pm S.E.M. Differences between means in two groups were carried out by a two-tailed Student's *t*-test. One-way analysis of variance (ANOVA) followed by Student–Newman–Keuls test was used to comparing differences between means in more than two groups. Influx studies were carried out by the two ways ANOVA followed by Student–Newman–Keuls test and data were presented as mean \pm S.D. A probability value of $P < 0.05$ was considered to be statistically significant.

3. Results

3.1. Effect of MPP⁺ on cell viability

To avoid the influence of reduced cell number on the following experiment, we first did the cell viability assay to select a MPP⁺ concentration that did not affect cell viability. The viability of cells treated with 5 μ mol/L MPP⁺ for 24 h was unchanged compared to that of the control. However, a significant reduction of cell viability was observed when cells were treated with 10–160 μ mol/L MPP⁺ (Fig. 1). Addition of the solvent alone had no effect on survival (data not shown). We also observed cell nuclear morphological

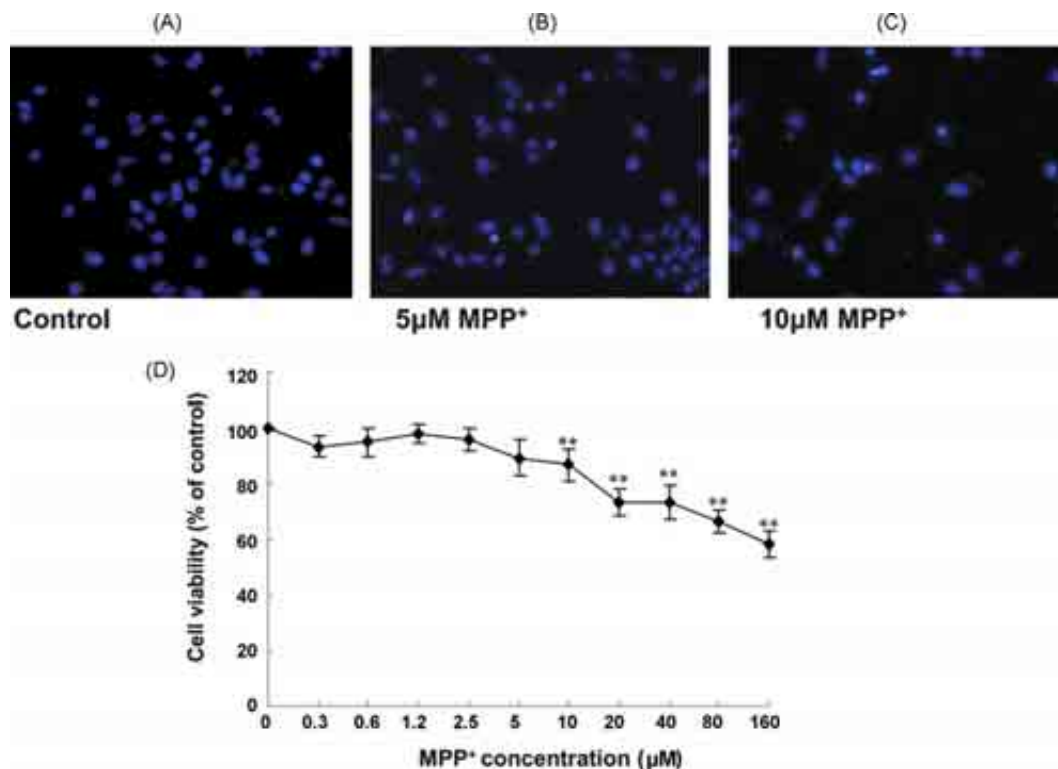


Fig. 1. MTT analysis of cell viability with MPP⁺ treatment. MES23.5 cell viability following MPP⁺ treatment was determined by MTT assay. The viability of cells treated with MPP⁺ (<5 μ mol/L) for 24 h was unchanged compared to that of control. A significant reduction of cell viability was observed when cells were treated with 10–160 μ mol/L MPP⁺. (A), (B), (C): Representative photographs of Hoechst 33258 staining from cells with different doses of MPP⁺ treatment. Magnification 200 \times . Data were presented as mean \pm S.E.M. of 6 independent experiments. ** $P < 0.01$, compared with the control.

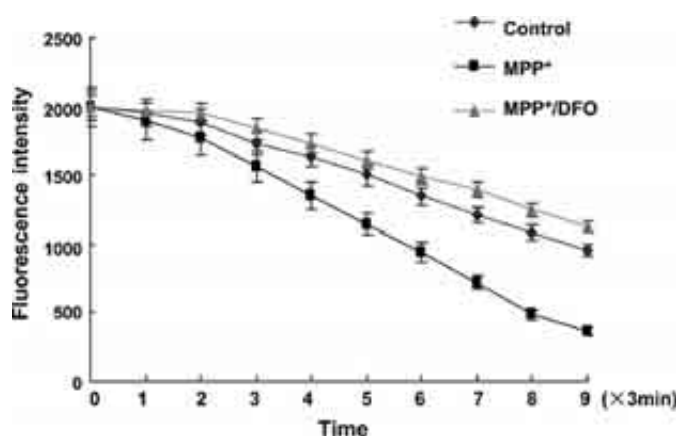


Fig. 2. Calcein-induced ferrous iron influx in MES23.5 cells. Ferrous iron influx into MES23.5 cells was determined by the quenching of calcein fluorescence, which is an indicator of intracellular iron level. The fluorescence intensity represented the mean value of 35 separate cells from four separate fields at each time point and was presented as mean \pm S.D. of 6 independent experiments. Cells treated with MPP⁺ showed more rapid and steady fluorescence quenching perfusing with 1 mmol/L ferrous in HBS compared to the control. The fluorescence intensity decreased rapidly, indicating the extracellular ferrous iron was transported into cells. Pretreatment with DFO (1 mmol/L, 2 h) before ferrous iron perfusion could completely block the fluorescence quenching. (Two-way ANOVA, MPP⁺ vs. control, $P < 0.01$; MPP⁺/DFO vs. MPP⁺, $P < 0.01$).

changes by using Hoechst 33258 staining. In agreement with the results of cell viability, 0.31–5 μ mol/L MPP⁺ did not affect the nuclear morphology (Fig. 1B). However, MPP⁺ (10–160 μ mol/L) treatment caused nuclear condensation as shown in Fig. 1C. Twenty-four-hour treatment with 5 μ mol/L MPP⁺ was chosen for further experiments.

3.2. MPP⁺ increased calcein-induced ferrous iron influx in MES23.5 cells

The ferrous iron influx of MES23.5 cells was measured after cells were treated with 5 μ mol/L MPP⁺ for 24 h. There was a significant decrease in the fluorescence intensity between MPP⁺-treated cells and the control when perfused with 1 mmol/L ferrous iron (Fig. 2). DFO treatment for 2 h caused an even more slowly but not significant decrease in the fluorescence intensity, compared to the control, since DFO was a strong iron chelator that binded iron easily. This indicated that cells incubated with MPP⁺ showed increased ferrous iron uptake.

3.3. MPP⁺ treatment with iron incubation induces decrease in mitochondrial membrane potential ($\Delta\psi_m$) and production of ROS in MES23.5 cells

In dopaminergic neurons, accessible ferrous iron can react with hydrogen peroxide produced during oxidative deamination of dopamine, producing reactive hydroxyl radicals, which are highly toxic to the cell function. We measured the mitochondrial membrane potential and ROS production

in MPP⁺-treated cells. Mitochondrial membrane potential changes are markers of mitochondria function and often associated with apoptosis. As shown in Fig. 3A and C, MPP⁺ itself had no effect on $\Delta\psi_m$. When MPP⁺-treated cells incubated in 100 μ mol/L ferrous iron for 3 h, they showed a significant 25% decrease of $\Delta\psi_m$. Pretreatment with DFO for 2 h could fully abolish this reduction. Cells solely incubated in 100 μ mol/L ferrous iron for 3 h only showed 12% reduction. The relationship between increased ferrous iron influx and decreased $\Delta\psi_m$ suggests that iron was involved in the MPP⁺-induced apoptosis through the mitochondria dysfunction. Since ROS play an important role in apoptosis and changes of mitochondrial membrane potential are considered to be involved in ROS production, we next investigated the intracellular ROS using a fluorescence sensitive probe (H₂DCF-DA) that detected various active oxygen species. As presented in Fig. 3B and D, there was a significant 69% increase in the level of ROS in MPP⁺-treated cells when incubated with ferrous iron, which could be totally suppressed by DFO pretreatment.

3.4. MPP⁺ treatment with iron incubation induces caspase-3 activation

Caspase-3 is a key protein in the process of apoptosis. Consistent with the above observation, activation of the effector caspases was also observed. The active caspase-3 was measured using the PE-conjugated monoclonal active caspase-3 antibody apoptosis kit. As shown in Fig. 4, cells incubated with ferrous iron after MPP⁺ treatment resulted in a 70% increase in the activated caspase-3, and this effect could be antagonized by DFO pretreatment. MPP⁺ treatment alone without ferrous iron incubation had no effect on caspase-3 activation. These results indicated that intracellular ferrous iron was responsible for MPP⁺-induced apoptosis in MES23.5 cells.

3.5. MPP⁺ treatment with iron incubation-induced DNA fragment of MES23.5 cells

Apoptosis was further confirmed by analyzing the nuclear morphology, which was evaluated with membrane-permeable blue Hoechst 33258. In control, Fe²⁺- and MPP⁺-treated groups, nuclei of MES23.5 cells appeared with regular contours and were round and large in size (Fig. 5). However, the nuclei of MPP⁺/Fe²⁺ group appeared hypercondensed (brightly stained). While pretreatment with DFO could significantly abolish ferrous iron-induced nuclear morphological changes.

3.6. MPP⁺-induced up-regulation of DMT1 (–IRE) expression, but not DMT1 (+IRE)

To find out whether this increased intracellular ferrous iron was due to the increased expression of DMT1, we

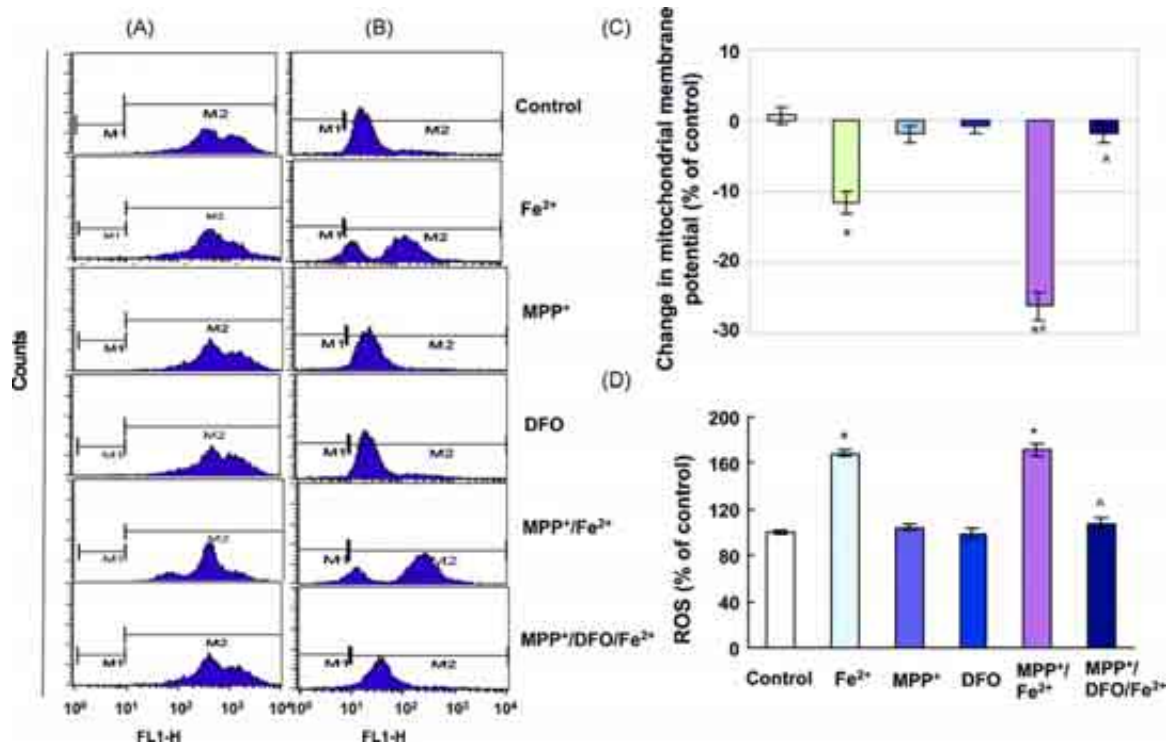


Fig. 3. MPP⁺ treatment with iron incubation decreased mitochondrial transmembrane potential ($\Delta\psi_m$) assessed by a fluorometric technique (see Section 2) after 24h exposure period (A and C), but no further increase in ROS production (B and D). Pretreatment with DFO fully abolished this increase. (A) Representatives of the fluorometric assay on $\Delta\psi_m$ of different groups. (B) Statistical analysis of the fluorometric assay on $\Delta\psi_m$ of different groups. (C) Representatives of the fluorometric assay on ROS of different groups. Statistical analysis was presented as (D). Data were presented as mean \pm S.E.M. of 3 independent experiments. Fluorescence values of the control were set to 100%. * $P < 0.01$, compared to the control. # $P < 0.01$, compared to Fe²⁺ group, ^ $P < 0.01$, compared to MPP⁺/Fe²⁺ group.

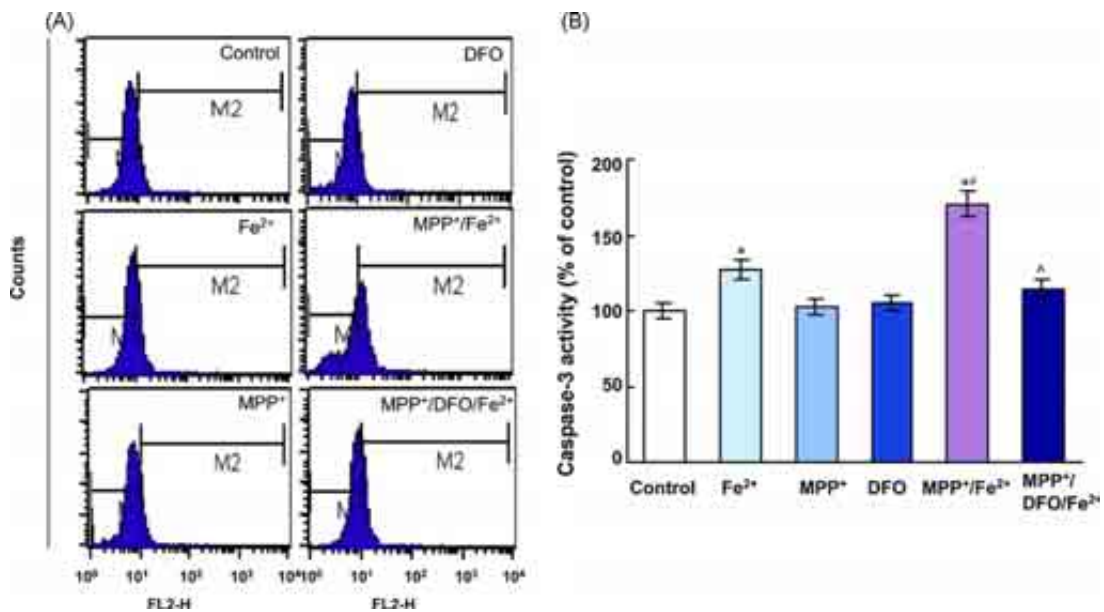


Fig. 4. Effect of MPP⁺ treatment with iron incubation on the activation of caspase-3 in MES23.5 cells. New DMEM/F12 with Fe²⁺ (100 μ mol/L) was applied for 3 h, after MPP⁺ (5 μ mol/L) treatment for 24 h. (A) Representatives of the fluorometric assay of active caspase-3 in different groups. (B) Statistical analysis. Data were presented as percentage of control and shown as mean \pm S.E.M. of 3 independent experiments. * $P < 0.05$, compared to the control. # $P < 0.01$, compared to Fe²⁺ group, ^ $P < 0.01$, compared to MPP⁺/Fe²⁺ group.

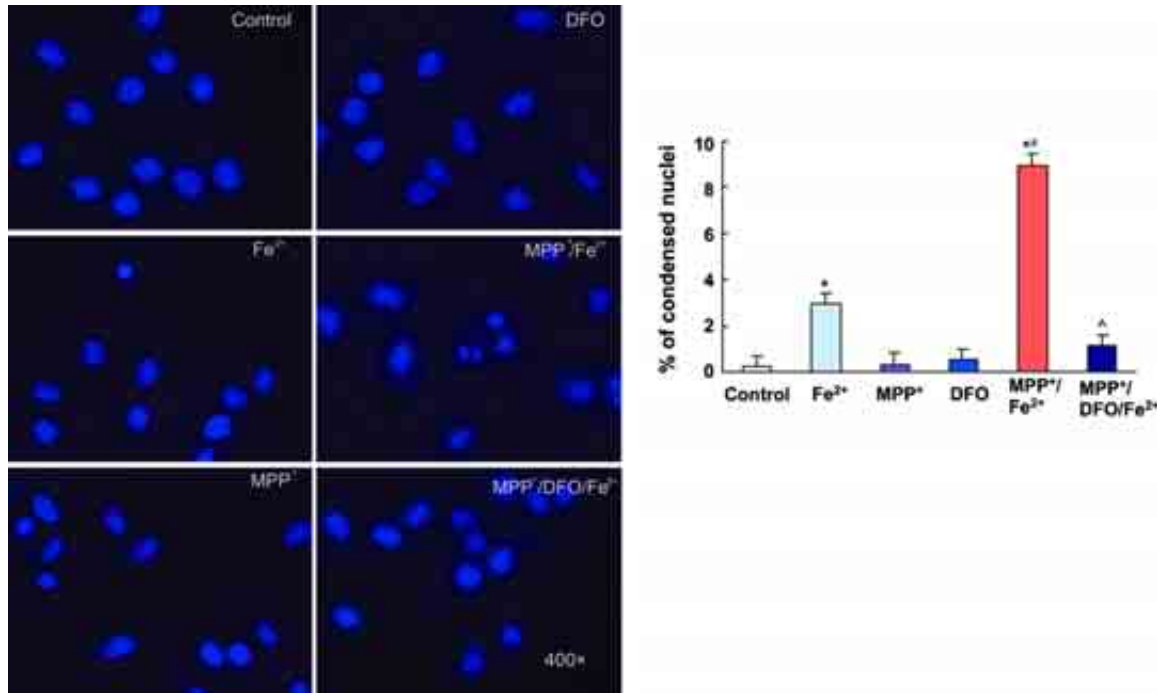


Fig. 5. Morphological changes in the nuclei of MES23.5 cells with different treatments. Cells in MPP⁺/Fe²⁺ group showed hypercondensed nuclear, while other groups showed no changes in nuclear morphology. Magnification 400×. *P < 0.05, compared to the control. #P < 0.01, compared to Fe²⁺ group, ^P < 0.01, compared to MPP⁺/Fe²⁺ group.

examined DMT1 (+IRE) and DMT1 (–IRE) expression levels by Western blots in MPP⁺-treated cells and the control. Only DMT1 (–IRE) protein in MPP⁺-treated MES23.5 cells was up-regulated to 50% compared to the control (Fig. 6), while there was no obvious change for DMT1 (+IRE).

To further investigate whether this increased DMT1 (–IRE) protein level was due to the increased DMT1 mRNA transcription, quantitative PCR was conducted to measure DMT1 mRNA levels. Similar to what we found at the protein level, there was a twofold increase of DMT1 (–IRE) mRNA, while DMT1 + IRE mRNA showed no change (Table 1). This indicates MPP⁺ treatment of MES23.5 cells will increase DMT1 (–IRE) expression in both mRNA and protein level.

3.7. Up-regulation of DMT1 is IRE/IRP-independent

Since IRP1 and IRP2 are the main proteins that register cytosolic iron concentration and post-transcriptionally regulate expression of iron metabolism genes, we examined their

expressions in Fe²⁺-, MPP⁺- and MPP⁺/Fe²⁺-treated cells. As shown in Fig. 7, ferrous iron itself used in our experiment did not have any effect on the expression of IRP1 and IRP2. In MPP⁺-treated cells, there were no changes for IRP1, whereas

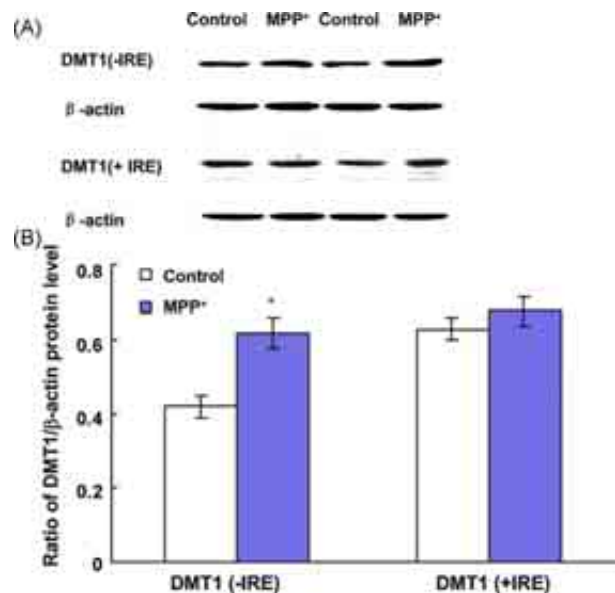


Fig. 6. MPP⁺ up-regulated DMT1 (–IRE) expression, but had no effect on DMT1 (+IRE). (A) Western blots were applied to detect DMT1 (–IRE) and DMT1 (+IRE). Increased expression of DMT1 (–IRE) was observed in MPP⁺-treated cells. β-actin was used as a loading control. (B) Statistical analysis. Data were presented as the ratio of DMT1 (+IRE) or DMT1 (–IRE) to β-actin. Each bar represented the mean ± S.E.M. of 6 independent experiments. *P < 0.05, compared to the control.

Table 1
Quantitative PCR analysis for DMT1 (+IRE) and DMT1 (–IRE) mRNA expression in MPP⁺-treated MES23.5 cells

	Mean ± S.E.M.	P value
DMT1 + IRE	+1.013 ± 0.145	>0.05
DMT1 – IRE	+2.117 ± 0.033	<0.05

Data were presented as mean ± S.E.M. of 6 independent experiments. It represented the fold changes of the mRNA expression with the treatment vs. the control in MES23.5 cells. ‘+’ indicated the up-regulation.

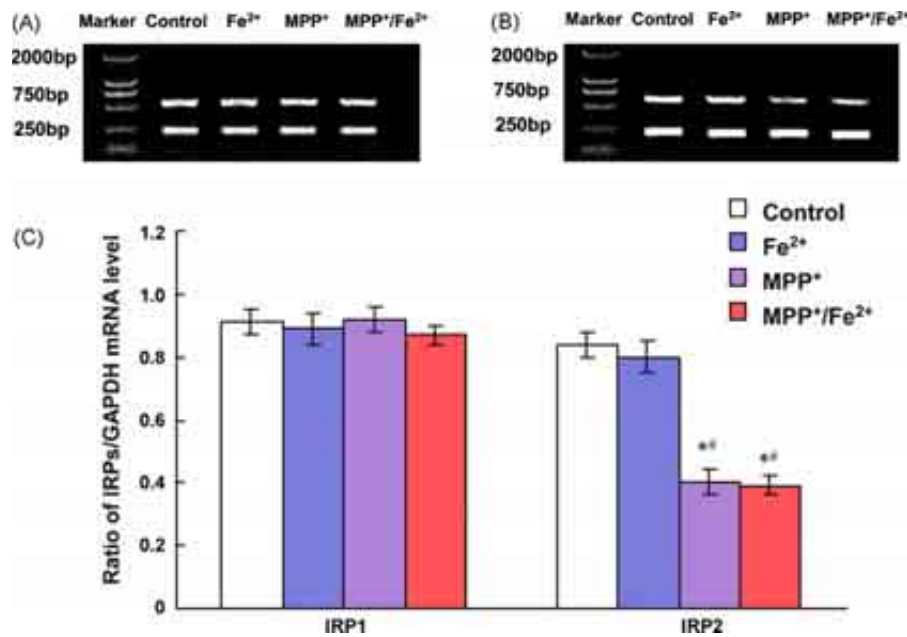


Fig. 7. Unchanged IRP1 and decreased IRP2 levels were observed in MES23.5 cells with iron incubation. (A) RT-PCR of IRP1 in the control, Fe²⁺-, MPP⁺- and MPP⁺/Fe²⁺-treated MES23.5 cells. Mouse GAPDH was used as a loading control. There were no significant differences among these groups. (B) RT-PCR of IRP2 in the control, Fe²⁺-, MPP⁺- and MPP⁺/Fe²⁺-treated MES23.5 cells. IRP2 mRNA was decreased in MPP⁺- and MPP⁺/Fe²⁺-treated groups. (C) Statistical analysis. Data were presented as the ratio of IRP1 or IRP2 to GAPDH. Each bar represented the mean \pm S.E.M. of 6 independent experiments. * $P < 0.05$, compared to the control, # $P < 0.05$, compared to Fe²⁺ group.

a significant decrease in IRP2 was observed. Similar results were observed for MPP⁺/Fe²⁺-treated cells. There was no difference between MPP⁺ and MPP⁺/Fe²⁺ groups, indicating the reduction of IRP2 mRNA expression was the effect of MPP⁺, not Fe²⁺. Since there is an IRE in the 3'-UTR of DMT1 (+IRE) mRNA, the unchanged expression of DMT1 (+IRE) and increased expression of DMT1 (-IRE) showed that their expressions are not controlled by IRP. This indicates an IRE/IRP-independent regulation is involved in this process.

4. Discussion

In this study we demonstrate the following findings. First, MPP⁺ treatment of MES23.5 cells will cause an increased ferrous iron influx. Second, this increased iron influx will damage the mitochondria function and increase ROS generation, which ultimately activates caspase-3, leading to the cell's apoptosis. Iron chelator DFO could prevent the iron-induced apoptosis. Third, MPP⁺-induced ferrous iron influx is due to the up-regulation of DMT1 (-IRE). Finally, this up-regulation is IRE/IRP-independent.

MES23.5 cells were used in this study because it obtains at least three neuronal features, namely, tyrosine hydroxylase, dopamine synthesis system, and omega-conotoxin receptor expression (Crawford et al., 1992). It exhibits several properties similar to the primary neurons originated from the SN. Therefore, the results from this cell line will give direct

evident correlation to the degenerated dopaminergic neurons in PD. Evidence for apoptosis of neurons has been described in the SN of patients with PD. MPTP is a well-established pro-toxin that causes the selective destruction of the SN in humans and other primates resulting in an acute Parkinsonism (Poirier et al., 1985; Temlett et al., 1994; Yang et al., 2007). MPTP-treated animals exhibit the major hallmarks of PD, including the loss of dopaminergic neurons in the SN. Furthermore, MPTP-induced toxicity mirrors the oxidative stress that plays a major role in the degeneration of dopaminergic neurons. MPTP is converted to its active MPP⁺ form by the monoamine oxidase B within glia. MPP⁺ is then taken up by dopaminergic neurons through the terminal receptor dopamine transporter. Upon entering the dopaminergic neurons, MPP⁺ will selectively damage mitochondria function and lead to cell demise. There are several evidences that iron is involved in the MPTP toxicity. High levels of iron have already been shown to be capable of catalyzing the oxidation of MPTP to MPP⁺ in solution producing both hydrogen peroxide and hydroxyl radicals and dopaminergic cell death following MPTP administration *in vivo* (Poirier et al., 1985; Temlett et al., 1994; Lan and Jiang, 1997). Our published study also showed increased iron levels in the SN in mice after MPTP administration *in vivo* (Jiang et al., 2003). However, how iron selectively aggregated in this specific area and through what mechanism iron enters the cell is far from known. Although there is some evidence that TfR may account for the iron uptake in MPP⁺ toxicity, the mechanism still needs further inves-

tigation since TfR only accounts for the transport of ferric iron. The most dangerous form of iron is its ferrous status; how this dangerous form of iron enters the cell requires elegant investigation. Up to now, the only known protein responsible for the ferrous iron transport is DMT1, therefore, we investigate its expression in MPP⁺-treated MES23.5 cells.

We found increased expression of DMT1, but only its –IRE form. This increased expression was due to transcriptional regulation, which was confirmed by real-time PCR. No changes were found in IRP1, but decreased expression of IRP2 was observed. This indicates that MPP⁺ treatment failed to activate IRP. In mammalian cells, IRP1 has retained its ability to function as an aconitase, whereas IRP2 is the chief physiologic iron sensor. The increased intracellular ferrous iron level may account for the decreased IRP2 expression. Decreased IRP2 will fail to bind the IRE in the 3′-UTR of the TfR mRNA and 5′-UTR of ferritin mRNA, causing the TfR transcript to become vulnerable to endonucleolytic cleavage, degeneration and formation and increased ferritin synthesis (Rouault, 2006). This is a cell-protective mechanism to produce less iron transporter and more iron storage protein. Although DMT1 contains an IRE in the 3′-UTR and this IRE is suggested to be functionally analogous to that located in the TfR mRNA, its function has never been proven and has been questioned (Wardrop and Richardson, 1999). No response of DMT1 (+IRE) to decreased IRP2 addresses this issue. This is in consensus with other studies. Ke et al. (2005) investigated the expression of two isoforms of DMT1 in different brain regions were affected by age, but not by iron status in adult rats. However, in the small intestine, DMT1 mRNA expression and protein level are negatively regulated by iron status. In hepatocytes, DMT1 expression and protein level were positively regulated by iron at the post-transcriptional level (Trinder et al., 2000). Since there are many controversial reports, further efforts are needed to clarify these issues. As DMT1 (–IRE) form contains no IRE in the 3′-UTR of its mRNA, the mechanism for current up-regulation is still unknown. There are many other factors that are involved in the regulation of DMT1 mRNA, such as two CCAAT boxes but lacking a TATA box, five potential metal response elements, three potential SP1 binding sites and a single γ -interferon regulatory element in its 5′-regulatory region (Lee et al., 1998); a lot of work needs to be done in the near future.

The increased intracellular ferrous iron will interact with hydrogen peroxide to form hydroxyl radicals, which causes the mitochondria dysfunction, indicated by our observed decreased mitochondria membrane potential. It is widely accepted that alterations in mitochondria function play an essential role in apoptosis. Cytochrome *c* release from the dysfunctional mitochondria, through different mechanisms, activates the executioner caspase, caspase-3, which cleaves PARP and activates endonucleases leading to DNA fragmentation (Bayir et al., 2006; Bredesen et al., 2006; Jantova et al., 2007). This is further confirmed by our data from using the

iron chelator that could fully abolish iron-induced apoptosis. These results are consistent with other studies (Kalivendi et al., 2003) and supported by the reports that iron chelators that are systemically administered to MPTP-treated rats prevent the progressive loss of dopaminergic neurons (Lan and Jiang, 1997). One research reported the iron chelator-brain selective MAO-AB inhibitor M30 could attenuate the DA depleting action of the neurotoxin and increase striatal levels of DA, 5-HT and NA in MPTP PD mice model (Gal et al., 2005), this might be the consequence of chelating increased iron-induced by MPTP.

In summary, in the present study we show that up-regulation of DMT1 (–IRE) accounts for the increased iron influx caused by MPP⁺ treatment. Our findings plus the results reported by the others show that iron is involved in MPP⁺-induced apoptosis. This apoptosis pathway is through the mitochondria dysfunction and activation of caspase-3.

Disclosure statement

There are no actual or potential conflicts of interest.

Acknowledgements

We thank Dr. Wei-dong Le to give us the MES23.5 cell line. This work was supported by the grants from the National Program of Basic Research sponsored by the Ministry of Science and Technology of China (2007CB516701, 2006CB500704), the National Foundation of Natural Science of China (Nos. 30400139 and 30570649) and Ministry of Education of China (20041065001).

References

- Andersen, J.K., 2004. Iron dysregulation and Parkinson's disease. *J. Alzheimers Dis.* 6, S47–S52.
- Andrews, N.C., Fleming, M.D., Gunshin, H., 1999. Iron transport across biologic membranes. *Nutr. Rev.* 57, 114–123.
- Bayir, H., Fadeel, B., Palladino, M.J., Witaspl, E., Kurnikov, I.V., Tyurina, Y.Y., Tyurin, V.A., Amoscato, A.A., Jiang, J., Kochanek, P.M., DeKosky, S.T., Greenberger, J.S., Shvedova, A.A., Kagan, V.E., 2006. Apoptotic interactions of cytochrome *c*: redox flirting with anionic phospholipids within and outside of mitochondria. *Biochim. Biophys. Acta* 1757, 648–659.
- Berg, D., Hochstrasser, H., 2006. Iron metabolism in Parkinsonian syndromes. *Mov. Disord.* 21, 1299–1310.
- Bredesen, D.E., Rao, R.V., Mehlen, P., 2006. Cell death in the nervous system. *Nature* 443, 796–802.
- Breuer, W., Epsztejn, S., Cabantchik, Z.I., 1995. Iron acquired from transferrin by K562 cells is delivered into a cytoplasmic pool of chelatable iron(II). *J. Biol. Chem.* 270, 24209–24215.
- Burdo, J.R., Menzies, S.L., Simpson, I.A., Garrick, L.M., Garrick, M.D., Dolan, K.G., Haile, D.J., Beard, J.L., Connor, J.R., 2001. Distribution of divalent metal transporter 1 and metal transport protein 1 in the normal and Belgrade rat. *J. Neurosci. Res.* 66, 1198–1207.

- Crawford Jr., G.D., Le, W.D., Smith, R.G., Xie, W.J., Stefani, E., Appel, S.H., 1992. A novel N18TG2 x mesencephalon cell hybrid expresses properties that suggest a dopaminergic cell line of substantia nigra origin. *J. Neurosci.* 12, 3392–3398.
- Deguil, J., Jailloux, D., Page, G., Fauconneau, B., Houeto, J.L., Philippe, M., Muller, J.M., Pain, S., 2007. Neuroprotective effects of pituitary adenylate cyclase-activating polypeptide (PACAP) in MPP(+)-induced alteration of translational control in Neuro-2a neuroblastoma cells. *J. Neurosci. Res.* 85, 2017–2025.
- Dexter, D.T., Wells, F.R., Lees, A.J., Agid, F., Agid, Y., Jenner, P., Marsden, C.D., 1989. Increased nigral iron content and alterations in other metal ions occurring in brain in Parkinson's disease. *J. Neurochem.* 52, 1830–1836.
- Dexter, D.T., Sian, J., Jenner, P., Marsden, C.D., 1993. Implications of alterations in trace element levels in brain in Parkinson's disease and other neurological disorders affecting the basal ganglia. *Adv. Neurol.* 60, 273–281.
- Gal, S., Zheng, H., Fridkin, M., Youdim, M.B., 2005. Novel multifunctional neuroprotective iron chelator-monoamine oxidase inhibitor drugs for neurodegenerative diseases. In vivo selective brain monoamine oxidase inhibition and prevention of MPTP-induced striatal dopamine depletion. *J. Neurochem.* 95, 79–88.
- Gotz, M.E., Double, K., Gerlach, M., Youdim, M.B., Riederer, P., 2004. The relevance of iron in the pathogenesis of Parkinson's disease. *Ann. NY Acad. Sci.* 1012, 193–208.
- Gunshin, H., Mackenzie, B., Berger, U.V., Gunshin, Y., Romero, M.F., Boron, W.F., Nussberger, S., Gollan, J.L., Hediger, M.A., 1997. Cloning and characterization of a mammalian proton-coupled metal-ion transporter. *Nature* 388, 482–488.
- Hardy, P.A., Gash, D., Yokel, R., Andersen, A., Ai, Y., Zhang, Z., 2005. Correlation of R2 with total iron concentration in the brains of rhesus monkeys. *J. Magn. Reson. Imaging* 21, 118–127.
- Huang, E., Ong, W.Y., Connor, J.R., 2004. Distribution of divalent metal transporter-1 in the monkey basal ganglia. *Neuroscience* 128, 487–496.
- Hubert, N., Hentze, M.W., 2002. Previously uncharacterized isoforms of divalent metal transporter (DMT)-1: implications for regulation and cellular function. *Proc. Natl. Acad. Sci. U.S.A.* 99, 12345–12350.
- Jantova, S., Cipak, L., Letasiova, S., 2007. Berberine induces apoptosis through a mitochondrial/caspase pathway in human promonocytic U937 cells. *Toxicol. In Vitro* 21, 25–31.
- Jiang, H., Qian, Z.M., Xie, J.X., 2003. Increased DMT1 expression and iron content in MPTP-treated C57BL/6 mice. *Sheng Li Xue Bao.* 55, 571–576.
- Jiang, H., Luan, Z., Wang, J., Xie, J., 2006. Neuroprotective effects of iron chelator Desferal on dopaminergic neurons in the substantia nigra of rats with iron-overload. *Neurochem. Int.* 49, 605–609.
- Jiang, H., Song, N., Wang, J., Ren, L.Y., Xie, J.X., 2007. Peripheral iron dextran induced degeneration of dopaminergic neurons in rat substantia nigra. *Neurochem. Int.*
- Kalivendi, S.V., Kotamraju, S., Cunningham, S., Shang, T., Hillard, C.J., Kalyanaraman, B., 2003. 1-Methyl-4-phenylpyridinium (MPP+)-induced apoptosis and mitochondrial oxidant generation: role of transferrin-receptor-dependent iron and hydrogen peroxide. *Biochem. J.* 371, 151–164.
- Kamp, D.W., Panduri, V., Weitzman, S.A., Chandel, N., 2002. Asbestos-induced alveolar epithelial cell apoptosis: role of mitochondrial dysfunction caused by iron-derived free radicals. *Mol. Cell Biochem.* 234–235, 153–160.
- Ke, Y., Chang, Y.Z., Duan, X.L., Du, J.R., Zhu, L., Wang, K., Yang, X.D., Ho, K.P., Qian, Z.M., 2005. Age-dependent and iron-independent expression of two mRNA isoforms of divalent metal transporter 1 in rat brain. *Neurobiol. Aging* 26, 739–748.
- Knutson, M., Menzies, S., Connor, J., Wessling-Resnick, M., 2004. Developmental, regional, and cellular expression of SFT/UbcH5A and DMT1 mRNA in brain. *J. Neurosci. Res.* 76, 633–641.
- Lan, J., Jiang, D.H., 1997. Desferrioxamine and vitamin E protect against iron and MPTP-induced neurodegeneration in mice. *J. Neural Transm.* 104, 469–481.
- Lee, P.L., Gelbart, T., West, C., Halloran, C., Beutler, E., 1998. The human Nramp2 gene: characterization of the gene structure, alternative splicing, promoter region and polymorphisms. *Blood Cells Mol. Dis.* 24, 199–215.
- Mackenzie, B., Takanaga, H., Hubert, N., Rolfs, A., Hediger, M.A., 2007. Functional properties of multiple isoforms of human divalent metal-ion transporter 1 (DMT1). *Biochem. J.* 403, 59–69.
- May, J.M., Qu, Z.C., Mendiratta, S., 1999. Role of ascorbic acid in transferrin-independent reduction and uptake of iron by U-937 cells. *Biochem. Pharmacol.* 57, 1275–1282.
- Moos, T., Morgan, E.H., 2004. The metabolism of neuronal iron and its pathogenic role in neurological disease: review. *Ann. NY Acad. Sci.* 1012, 14–26.
- Picard, V., Govoni, G., Jabado, N., Gros, P., 2000. Nramp 2 (DCT1/DMT1) expressed at the plasma membrane transports iron and other divalent cations into a calcein-accessible cytoplasmic pool. *J. Biol. Chem.* 275, 35738–35745.
- Poirier, J., Donaldson, J., Barbeau, A., 1985. The specific vulnerability of the substantia nigra to MPTP is related to the presence of transition metals. *Biochem. Biophys. Res. Commun.* 128, 25–33.
- Riederer, P., Sofic, E., Rausch, W.D., Schmidt, B., Reynolds, G.P., Jellinger, K., Youdim, M.B., 1989. Transition metals, ferritin, glutathione, and ascorbic acid in parkinsonian brains. *J. Neurochem.* 52, 515–520.
- Rouault, T.A., 2001. Iron on the brain. *Nat. Genet.* 28, 299–300.
- Rouault, T.A., 2006. The role of iron regulatory proteins in mammalian iron homeostasis and disease. *Nat. Chem. Biol.* 2, 406–414.
- Ryu, J.W., Hong, K.H., Maeng, J.H., Kim, J.B., Ko, J., Park, J.Y., Lee, K.U., Hong, M.K., Park, S.W., Kim, Y.H., Han, K.H., 2004. Overexpression of uncoupling protein 2 in THP1 monocytes inhibits beta2 integrin-mediated firm adhesion and transendothelial migration. *Arterioscler. Thromb. Vasc. Biol.* 24, 864–870.
- Sanelli, T., Ge, W., Leystra-Lantz, C., Strong, M.J., 2007. Calcium mediated excitotoxicity in neurofilament aggregate-bearing neurons in vitro is NMDA receptor dependant. *J. Neurol. Sci.* 256, 39–51.
- Song, N., Jiang, H., Wang, J., Xie, J.X., 2007. Divalent metal transporter 1 up-regulation is involved in the 6-hydroxydopamine-induced ferrous iron influx. *J. Neurosci. Res.* 85, 3118–3126.
- Temlett, J.A., Landsberg, J.P., Watt, F., Grime, G.W., 1994. Increased iron in the substantia nigra compacta of the MPTP-lesioned hemiparkinsonian African green monkey: evidence from proton microprobe elemental microanalysis. *J. Neurochem.* 62, 134–146.
- Tenopoulou, M., Doulias, P.T., Barbouti, A., Brunk, U., Galaris, D., 2005. Role of compartmentalized redox-active iron in hydrogen peroxide-induced DNA damage and apoptosis. *Biochem. J.* 387, 703–710.
- Trinder, D., Oates, P.S., Thomas, C., Sadleir, J., Morgan, E.H., 2000. Localisation of divalent metal transporter 1 (DMT1) to the microvillus membrane of rat duodenal enterocytes in iron deficiency, but to hepatocytes in iron overload. *Gut* 46, 270–276.
- Wang, J., Jiang, H., Xie, J.X., 2004. Time dependent effects of 6-OHDA lesions on iron level and neuronal loss in rat nigrostriatal system. *Neurochem. Res.* 29, 2239–2243.
- Wang, J., Jiang, H., Xie, J.X., 2007. Ferroportin 1 and hephaestin are involved in the nigral iron accumulation of 6-OHDA-lesioned rats. *Eur. J. Neurosci.* 25, 2766–2772.
- Wardrop, S.L., Richardson, D.R., 1999. The effect of intracellular iron concentration and nitrogen monoxide on Nramp2 expression and non-transferrin-bound iron uptake. *Eur. J. Biochem.* 263, 41–49.
- West, M.J., Slomianka, L., Gundersen, H.J., 1991. Unbiased stereological estimation of the total number of neurons in the subdivisions of the rat hippocampus using the optical fractionator. *Anat. Rec.* 231, 482–497.
- Wetli, H.A., Buckett, P.D., Wessling-Resnick, M., 2006. Small-molecule screening identifies the selanzal drug ebisen as a potent inhibitor of DMT1-mediated iron uptake. *Chem. Biol.* 13, 965–972.

- Xie, J., Jiang, H., Chen, W.F., Qian, Z.M., 2003. Dopamine release rather than content in the caudate putamen is associated with behavioral changes in the iron rat model of Parkinson's disease. *Exp. Neurol.* 182, 483–489.
- Yang, J., Su, Y., Richmond, A., 2007. Antioxidants tiron and *N*-acetyl-L-cysteine differentially mediate apoptosis in melanoma cells via a reactive oxygen species-independent NF-kappaB pathway. *Free Radic. Biol. Med.* 42, 1369–1380.
- Yao, G., Yang, L., Hu, Y., Liang, J., Hou, Y., 2006. Nonylphenol-induced thymocyte apoptosis involved caspase-3 activation and mitochondrial depolarization. *Mol. Immunol.* 43, 915–926.
- Zhu, H.J., Liu, G.Q., 2004. Glutamate up-regulates P-glycoprotein expression in rat brain microvessel endothelial cells by an NMDA receptor-mediated mechanism. *Life Sci.* 75, 1313–1322.